ATMIN Is Required for Maintenance of Genomic Stability and Suppression of B Cell Lymphoma

Joanna I. Loizou,[1] Rocio Sancho,[1] Nnennaya Kanu,[1] Daniel J. Bolland,[2] Fengtang Yang,[3] Cristina Rada,[4] Anne E. Corcoran,[2] and Axel Behrens[1,*]

[1]Mammalian Genetics Lab, Cancer Research UK, London Research Institute, 44, Lincoln's Inn Fields, London WC2A 3LY, UK
[2]The Babraham Institute, Laboratory of Chromatin and Gene Expression, Cambridge CB22 3AT, UK
[3]Wellcome Trust Sanger Institute, Wellcome Trust Genome Campus, Hinxton, Cambridge CB10 1SA, UK
[4]Medical Research Council Laboratory of Molecular Biology, Hills Road, Cambridge CB2 0QH, UK
*Correspondence: axel.behrens@cancer.org.uk
DOI 10.1016/j.ccr.2011.03.022

SUMMARY

Defective V(D)J rearrangement of immunoglobulin heavy or light chain (IgH or IgL) or class switch recombination (CSR) can initiate chromosomal translocations. The DNA-damage kinase ATM is required for the suppression of chromosomal translocations but ATM regulation is incompletely understood. Here, we show that mice lacking the ATM cofactor ATMIN in B cells (ATMIN$^{\Delta B/\Delta B}$) have impaired ATM signaling and develop B cell lymphomas. Notably, ATMIN$^{\Delta B/\Delta B}$ cells exhibited defective peripheral V(D)J rearrangement and CSR, resulting in translocations involving the *Igh* and *Igl* loci, indicating that ATMIN is required for efficient repair of DNA breaks generated during somatic recombination. Thus, our results identify a role for ATMIN in regulating the maintenance of genomic stability and tumor suppression in B cells.

INTRODUCTION

ATM is the protein kinase that is mutated in the hereditary autosomal-recessive disease ataxia telangiectasia (A-T) (Savitsky et al., 1995). A-T patients display immune deficiencies, cancer predisposition, neuronal degeneration, and radiosensitivity (McKinnon, 2004). The molecular role of ATM is to respond to DNA double-strand breaks (DSBs) and alterations in chromatin structure by phosphorylating its substrates, thereby promoting repair of damage or arresting the cell cycle (Xu and Baltimore, 1996). ATM is activated by two known cofactors in a stimulus-dependent manner. Following the induction of DSBs by ionizing radiation (IR), NBS1 (mutated in Nijmegen breakage syndrome) is required for activation of ATM. NBS1 activates ATM as part of the MRN complex that consists of Mre11 (the exonuclease mutated in ataxia telangiectasia-like disorder, ATLD) (D'Amours and Jackson, 2002; Stracker et al., 2004), Rad50, and NBS1 (Lee and Paull, 2004; Uziel et al., 2003).

ATM can also be activated in the absence of DNA damage. Treatment of cultured cells with hypotonic stress or chloroquine leads to the activation of ATM, presumably because these agents induce changes in chromatin structure (Bakkenist and Kastan, 2003). NBS1 null B cells are defective in ATM-dependent signaling following IR, but they show a functional ATM-signaling pathway in response to osmotic stress (Difilippantonio et al., 2005). We have recently described a second ATM cofactor, ATMIN for ATM interactor (Kanu and Behrens, 2007), also called ASCIZ for ATM/ATR-Substrate Chk2-Interacting zinc finger protein (McNees et al., 2005; Oka et al., 2008). ATMIN interacts with ATM using a motif homologous to that of NBS1 and in doing so stabilizes ATM at the protein level (Kanu and Behrens, 2007). ATMIN has a complementary function to NBS1 with respect to ATM activation: ATMIN is dispensable for IR-induced ATM signaling, but ATM activation following chloroquine treatment and hypotonic stress is mediated by ATMIN (Kanu and Behrens, 2007). Hence, NBS1 and ATMIN are required for ATM activation in a signal-dependent manner.

Significance

The DNA-damage kinase ATM has important functions in the suppression of chromosomal translocations and the prevention of lymphoid cancers. We have recently identified ATMIN as an ATM cofactor required for ATM function in a stimulus-dependent manner. Using conditional inactivation of ATMIN in B cells, we demonstrate that ablation of ATMIN-dependent noncanonical ATM activation results in oncogenic chromosomal translocations and subsequent tumor development. These translocations occur because programmed breaks generated during somatic recombination are not repaired effectively, leading to a defect in class switch recombination and genomic instability. Furthermore, B cell maturation is affected, and there is severe defect in ATM signaling. These findings indicate that noncanonical ATM activation is absolutely required for ATM function in cancer suppression.

In addition to functioning as an ATM cofactor, ATMIN has also been implicated in the DNA-damage response because it forms Rad51-containing foci in response to DNA-methylating agents, but not in response to DSB-inducing agents (McNees et al., 2005). Furthermore, ATMIN-deficient chicken DT40 B lymphocytes display markedly increased *Ig* gene conversion rates; however, neither the efficiency of DSB repair nor hypermutation was affected by ATMIN levels, indicating that ATMIN does not directly control homologous recombination or formation of abasic sites (Oka et al., 2008).

Physiologically, DNA DSBs are generated in the immune system during V(D)J recombination by the recombination activating gene 1/2 (RAG1/2) enzymes. During the maturation of B cells, DSBs also occur during class switch recombination (CSR) in a manner that is dependent on activation-induced cytidine deaminase (AID). DNA DSBs generated during both V(D)J recombination and CSR rely on nonhomologous end-joining (NHEJ) to repair the lesions. Indeed, both A-T patients and mice lacking ATM function are immunocompromised and develop leukemia and/or lymphoma (Barlow et al., 1996; Callen et al., 2007b; Camacho et al., 2002; Fang et al., 2003; Haidar et al., 2000; Schaffner et al., 1999, 2000; Stankovic et al., 2002; Stilgenbauer et al., 1999; Xu and Baltimore, 1996). Because the knockout mouse for ATM (ATM$^{-/-}$) recapitulates many of the immune defects exhibited by A-T patients, it is a good model to study the functions of ATM in the immune system. Specifically for B cells, ATM$^{-/-}$ mice have decreased pre-B cells in the bone marrow (BM), which is not attributed to fewer progenitors because similar numbers of less mature pro-B cells were present in the BM (Xu et al., 1996). It should be noted that despite this mild developmental defect of B cells, ATM$^{-/-}$ mice display normal numbers of mature B cells in the spleen (Xu et al., 1996).

AID is the enzyme that initiates both somatic hypermutation (SHM) and CSR (Muramatsu et al., 2000; Revy et al., 2000) by deaminating cytidines (Petersen-Mahrt et al., 2002). The deaminated cytidines can either lead to mutations associated with the variable region of *Igh* or to DSBs within the switch region that initiate CSR (Neuberger et al., 2003). CSR is reduced by about 75% in ATM$^{-/-}$ mice (Lumsden et al., 2004; Reina-San-Martin et al., 2004). Conversely, SHM is not affected upon deletion of ATM (Reina-San-Martin et al., 2004), and this is thought to be because such lesions are repaired through mismatch repair (MMR) and base excision repair (BER), which are ATM independent. A final phenotype of ATM$^{-/-}$ B cells is loss of genomic stability not only of chromosome 12 (which carries the *Igh* locus) but also of other loci (Callen et al., 2007b), indicating that ATM functions in the repair of breaks specifically generated during CSR within the *Igh* locus but also in maintaining general genomic stability.

Some of the defects displayed in ATM$^{-/-}$ mice are not entirely recapitulated upon deletion of NBS1 in various mouse models. Whereas the deletion of NBS1 in B cells leads to a reduced efficiency in CSR, the defect is less pronounced than that displayed by ATM mutants (Kracker et al., 2005; Lumsden et al., 2004; Reina-San-Martin et al., 2004). Also, in a mouse model harboring mutations within NBS1 that are found in patients with NBS (hNbs1$^{657\Delta 5}$), the development of B cell and T cell lymphoma occurred only in a p53 null (p53$^{-/-}$) background (Difilippantonio et al., 2005), whereas ATM$^{-/-}$ mice develop thymomas with high penetrance (Xu et al., 1996). Furthermore, homozygous knock-in mice harboring a deletion of ATM that commonly occurs in A-T patients (7636 del9 mutation) did develop B cell lymphoma (Spring et al., 2001), indicating a role for ATM in the suppression of B cell lymphoma in mice. Hence, the data from both cellular models and in vivo models for ATM and NBS1 indicate a possible role for MRN-independent activation of ATM.

Although DNA damage-independent ATM activation has been observed in cultured cells, the physiological relevance of ATMIN-regulated chromatin-induced ATM activation was unknown. In this study we test the functional significance of noncanonical ATM signaling in B cells.

RESULTS

ATMIN Is Required during B Cell Maturation

Due to the embryonic lethality of ATMIN knockout mice (Kanu et al., 2010), we generated a conditional knockout mouse model for ATMIN in order to determine whether ATMIN is required for any of the functions of ATM in B cells. To delete ATMIN in B cells, we have flanked exon 4 of the *atmin* gene with loxP sites by targeted mutation of the *atmin* locus (ATMIN$^{F/F}$ mice) (see Figure S1A available online). Exon 4 encodes a large portion of the ATMIN protein (615 of 823 amino acids in murine ATMIN). We have previously described that mouse embryonic fibroblasts (MEFs) derived from mice with a homozygous germline deletion of *atmin* exon 4 do not express detectable ATMIN protein (Kanu and Behrens, 2007). Thus, deletion of *atmin* exon 4 generates a null mutation. By expressing cre-recombinase under the control of the CD19 promoter, ATMIN was deleted from the pro-B cell stage of development onward (denoted as ATMIN$^{\Delta B/\Delta B}$).

Recombination of the floxed *atmin* locus by CD19-cre was confirmed by PCR designed to identify the wild-type (WT), floxed, and deleted alleles in tail, spleen, BM, and thymus samples (Figure 1A). Absence of ATMIN protein and mRNA in B cells was additionally confirmed by western blot and quantitative RT-PCR, respectively, of ATMIN$^{F/F}$ and ATMIN$^{\Delta B/\Delta B}$-purified splenic B cells (Figures 1B and 1C).

In order to determine a possible role for ATMIN in the maturation of B cells, we analyzed cells from BM and spleen by FACS in parallel with WT and ATM$^{-/-}$ mice. Pre-B cells (B220$^+$CD43$^-$IgM$^-$) and immature B cells (B220$^+$CD43$^-$IgM$^+$) were decreased in ATMIN$^{\Delta B/\Delta B}$ and ATM$^{-/-}$ mice compared with their littermate controls (Figures 1D and 1E). Recirculating mature B cells in BM (B220^{hi}CD43$^-$IgM$^+$) were not significantly changed in ATMIN$^{\Delta B/\Delta B}$ and ATM$^{-/-}$ mice compared with littermate controls (Figures 1D and 1E). The FACS profiles of B220 and CD43 staining of pro-B BM cells are shown in Figures S1B and S1C. FACS analysis of CD43$^-$ (from Figures S1B and S1C) BM cells stained for B220 and IgM to identify pre-B cells, immature B cells, and recirculating mature B cells for the individual mice in Figures 1D and 1E is shown in Figures S1D and S1E. Analysis of the spleen revealed normal cellularity, normal frequency of peripheral splenic mature B cells (B220$^+$IgM$^+$), and normal total numbers of peripheral splenic mature B cells (B220$^+$IgM$^+$) in ATMIN$^{\Delta B/\Delta B}$ and/or ATM$^{-/-}$ mutant mice (Figures S1F–S1I). Furthermore, ATMIN$^{\Delta B/\Delta B}$ mice did not display a change in the structure of the spleen by hematoxylin and eosin staining (H&E) (Figure S1J). Thus, the phenotypes of ATMIN and ATM deficiency in B cell development share some similarities.
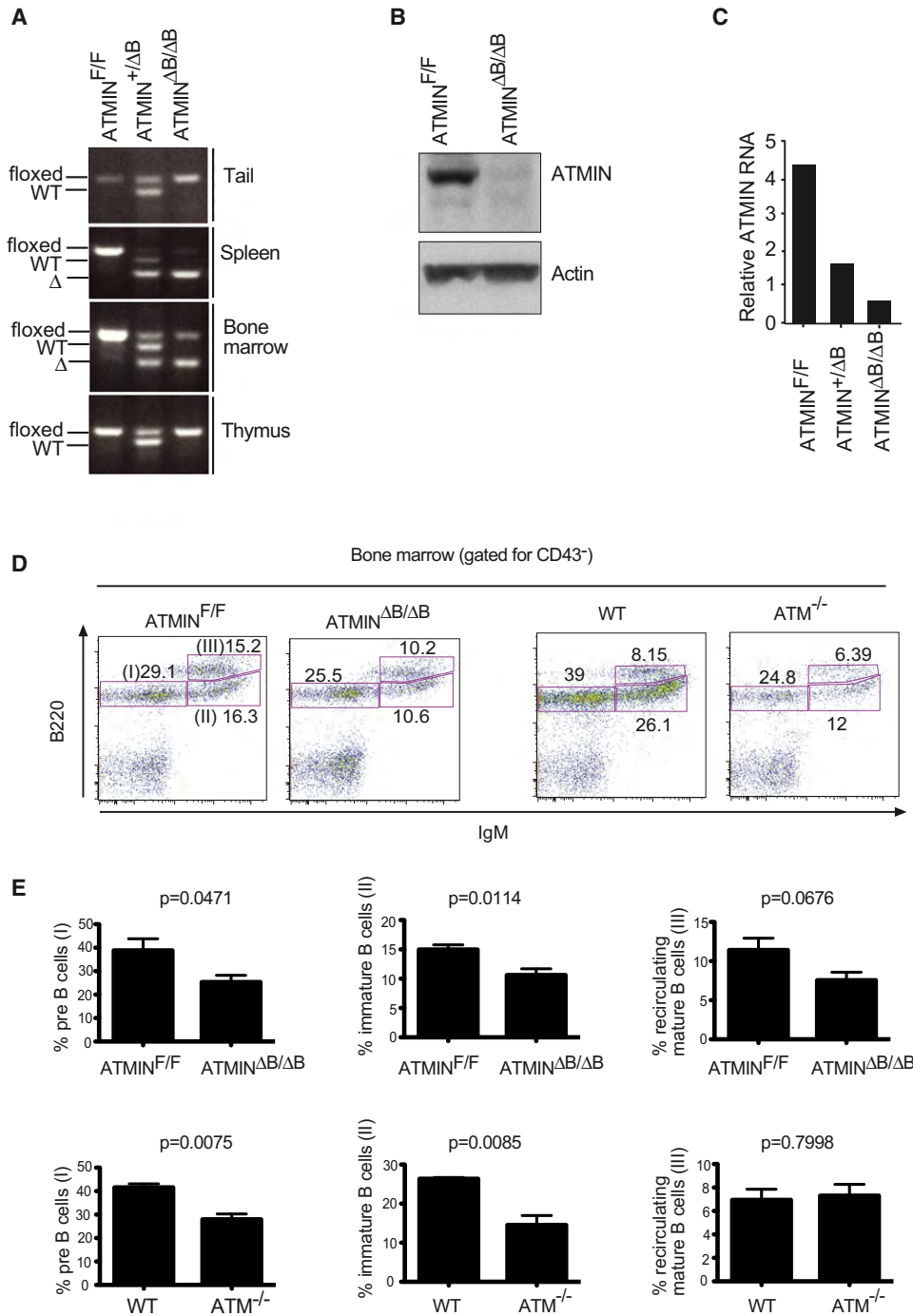
Figure 1. ATMIN Is Required during B Cell Maturation

(A) Genotyping of *atmin* WT, floxed, and Δ alleles by PCR from tail, spleen, BM, and thymus of ATMIN$^{F/F}$, ATMIN$^{+/ΔB}$, and ATMIN$^{ΔB/ΔB}$ mice.

(B) ATMIN is deleted in B cells from ATMIN$^{ΔB/ΔB}$ mice. Purified B lymphocytes from the spleen of ATMIN$^{F/F}$ and ATMIN$^{ΔB/ΔB}$ mice were blotted with anti-ATMIN and anti-β-actin antibodies.

(C) To assess ATMIN mRNA levels in B cells of ATMIN$^{F/F}$, ATMIN$^{+/ΔB}$, and ATMIN$^{ΔB/ΔB}$ mice, B cells were sorted as B220$^+$ and then RNA was extracted. Levels of ATMIN mRNA were normalized to actin.

(D) Pre-B cells (B220$^+$CD43$^-$IgM$^-$) denoted as "(I)" and immature B cells (B220$^+$CD43$^-$IgM$^+$) denoted as "(II)" are reduced in ATMIN$^{ΔB/ΔB}$ (n = 5) and ATM$^{-/-}$ (n = 3) BM, compared with their controls. Recirculating immature B cells (B220^{hi}CD43$^-$IgM$^+$) denoted as "(III)" are unchanged in ATMIN$^{ΔB/ΔB}$ (n = 5) and ATM$^{-/-}$ (n = 3) BM, as determined by FACS.

(E) Quantification of (D). Data are presented as mean and SD. Statistical analyses were calculated by a Student's t test with two-tailed distribution. p values are indicated.
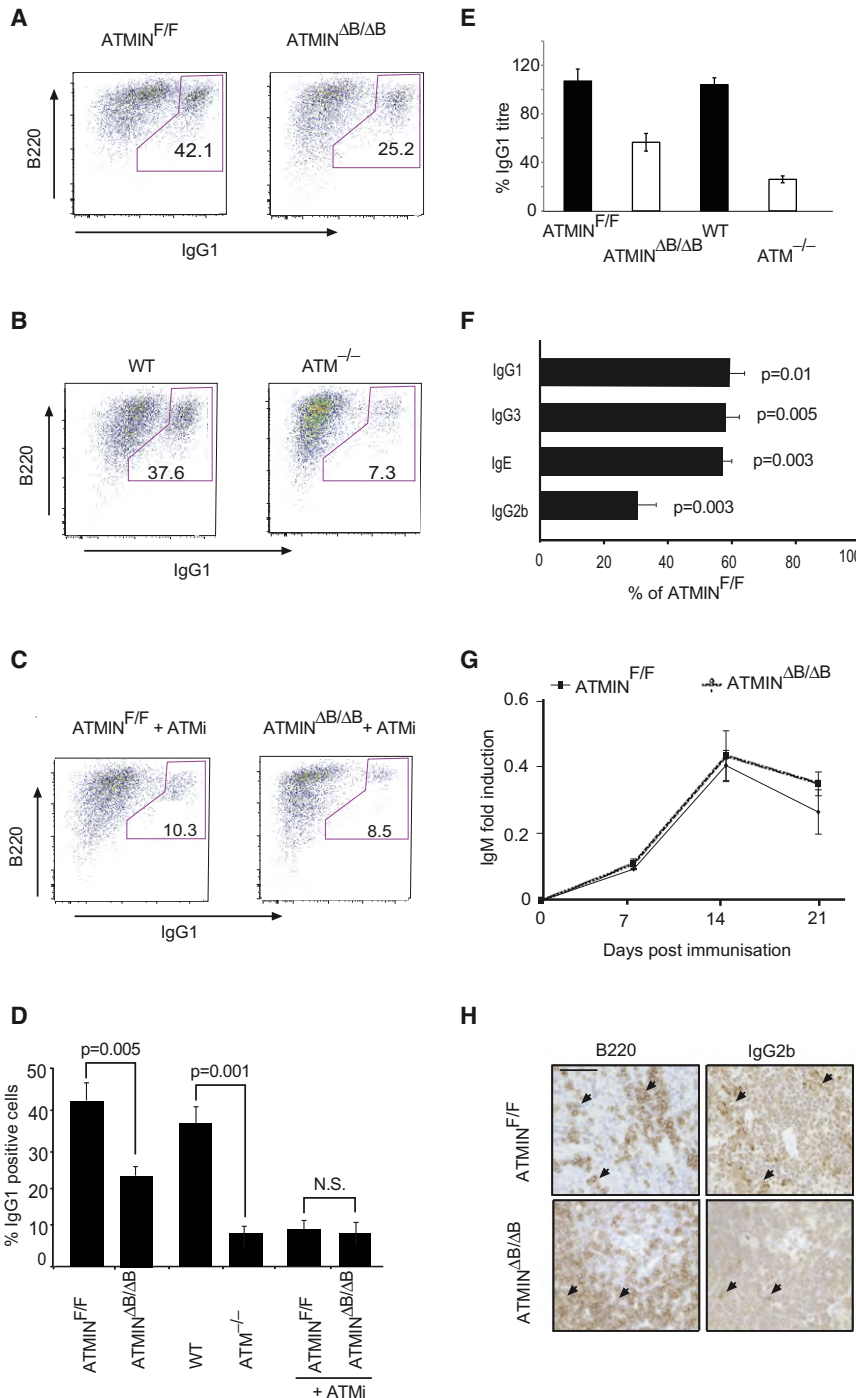
See also Figure S1.

Figure 2. CSR Is Perturbed in ATMIN$^{\Delta B/\Delta B}$ B Lymphocytes

(A) ATMIN$^{F/F}$ and ATMIN$^{\Delta B/\Delta B}$ or (B) WT and ATM$^{-/-}$-purified splenic B lymphocytes were stimulated with LPS/IL4 for 3 days and then stained with anti B220 and IgG1 (n = 4 per genotype).

(C) ATMIN$^{F/F}$ and ATMIN$^{\Delta B/\Delta B}$-purified splenic B lymphocytes were stimulated with LPS/IL4 for 3 days in the presence of an ATM inhibitor (ATMi) and then stained with anti B220 and IgG1 (n = 4 per genotype).

(D) Data from (A)–(C) are presented as mean and SD. Statistical analyses were calculated by a Student's t test with two-tailed distribution. p values are indicated. N.S., not significant.

(E) Splenic B cells were purified from ATMIN$^{F/F}$, ATMIN$^{\Delta B/\Delta B}$, WT, and ATM$^{-/-}$ mice and stimulated with LPS/IL4 for 6 days following which supernatants were analyzed for IgG1 by ELISA (n = 3 per genotype). Error bars denote SD.

(F) ATMIN$^{F/F}$ and ATMIN$^{\Delta B/\Delta B}$ mice (n = 4 per genotype) were immunized with TNP/KLH in FCA, serum was collected 7 days after a second immunization, and levels of antigen-specific Igs were assayed by ELISA. Significant decreases were observed between the levels of immunoglobulins in ATMIN$^{F/F}$ mice compared with ATMIN$^{\Delta B/\Delta B}$ mice. Data presented as mean and SD. Statistical analyses were calculated by a Student's t test with two-tailed distribution. p values are indicated.

(G) Mice were immunized as in (F), but levels of antigen-specific IgM were measured at the indicated time points after the first immunization (n = 4 per genotype). Error bars denote SD. No significant differences were observed between ATMIN$^{F/F}$ and ATMIN$^{\Delta B/\Delta B}$ mice calculated by a Student's t test with two-tailed distribution.

(H) Mice (n = 4 per genotype) were immunized as in (F) and culled 7 days after the second immunization following which the spleens were fixed and stained for B220 and IgG2b in serial sections. Arrowheads indicate regions of colocalization between B220 and IgG2b. Scale bar, 75 μm.
See also Figure S2.

process. During CSR AID initiates DSBs in both Sμ and a downstream S region, which are then joined by NHEJ. To determine whether ATMIN is required for CSR, we measured the surface expression of IgG1 on B cells following stimulation with LPS/IL4. In comparison to ATMIN$^{F/F}$ B cells, ATMIN$^{\Delta B/\Delta B}$ B cells displayed

Efficient CSR Is Dependent on ATMIN

Although it is clear that treatment of cultured cells with hypotonic stress or chloroquine leads to ATM activation (Bakkenist and Kastan, 2003), the physiological relevance of noncanonical ATM activation mimicked by these rather artificial conditions is not known. Because ATM is required for efficient CSR, and because chromatin structure is altered during CSR, we tested whether ATMIN may function as a cofactor for ATM in this

a 50% reduction in the efficiency of CSR (Figure 2A). As a control experiment, we stimulated ATMIN$^{F/F}$ and ATMIN$^{\Delta B/\Delta B}$ B cells with LPS/IL4 and observed that cells from both genotypes formed blasts with equal efficiency (Figures S2A and S2B) and displayed comparable cell-cycle profiles (Figures S2C and S2D). Furthermore, ATMIN$^{\Delta B/\Delta B}$ B cells stimulated with LPS/IL4 proliferated efficiently (as measured by dilution of CFSE) (Figure S2E) and did not undergo increased apoptosis, as measured

using subG1 analysis (Figure S2F) as well as TMRE and TOPRO staining (living cells are TMRE⁺TOPRO⁻) (Figure S2G), compared with ATMIN$^{F/F}$ B cells. These data indicate that the reduced efficiency of CSR is not a secondary consequence of altered cell proliferation or death but rather reflects a defect in recombination.

In order to address whether ATMIN functions in CSR through ATM, we assessed the amount of CSR in WT and ATM$^{-/-}$ cells and found this to be reduced about 75% (Figure 2B), and this defect was reproducible upon the treatment of ATMIN$^{F/F}$ B cells with an ATM small molecule inhibitor (ATMi; Ku55933) (Hickson et al., 2004) (Figure 2C). ATMi treatment reduced CSR to the same extent in ATMIN$^{\Delta B/\Delta B}$ and control B cells, indicating that ATMIN and ATM deficiency does not result in an additive defect in CSR (Figures 2C and 2D).

To ensure that the defect in CSR was not due to a delay in this process, we induced switching to either IgG1 (Figure S2H) or IgG3 (Figure S2I) by treating cells with CD40/IL4 or LPS for 5 days, respectively. Indeed, even after 5 days of CSR induction, ATMIN$^{\Delta B/\Delta B}$ B cells maintained a 50% defect in switching. In line with these data, ELISA revealed a 50% and 70% reduction in the amount of IgG1 secreted into the supernatant of the ATMIN$^{\Delta B/\Delta B}$ and ATM$^{-/-}$ B cell cultures, respectively, in comparison to that of the relative control cultures (Figure 2E).

To further confirm a CSR defect upon deletion of ATMIN, we measured the γ1 germline transcript (GLT), γ1 productive transcript (PT), and the γ1 circle transcript (CT) (Figure S2J). Whereas the γ1 GLT in ATMIN$^{\Delta B/\Delta B}$ cells was not significantly altered, the PT was greatly reduced in stimulated ATMIN$^{\Delta B/\Delta B}$ B cells (Figure S2K) as was the IgG1 CT (Figure S2L), further indicating that ATMIN functions in the process of CSR in vitro. The decrease in IgG1 CT in ATMIN$^{\Delta B/\Delta B}$ B cells cultures was also maintained when normalized to the B cell-specific gene Pax5 (Figure S2M).

To determine whether ATMIN is also required for CSR in vivo, we immunized ATMIN$^{F/F}$ and ATMIN$^{\Delta B/\Delta B}$ mice with the antigen TNP-KLH and then measured the amount of antigen-specific antibodies in the serum of the mice by ELISA. ATMIN$^{\Delta B/\Delta B}$ mice displayed a 45%–65% reduction in CSR to IgG1, IgG3, IgE, and IgG2b in comparison to ATMIN$^{F/F}$ mice (Figure 2F), whereas the levels of IgM were slightly elevated in ATMIN$^{\Delta B/\Delta B}$ compared with ATMIN$^{F/F}$ mice (Figure 2G). In addition we observed decreased staining for IgG2b (Figure 2H) in the spleens of ATMIN$^{\Delta B/\Delta B}$ mice compared with both ATMIN$^{F/F}$ mice post-stimulation with the antigen TNP-KLH. Taken together, the in vitro and in vivo data identify a role for MRN-independent noncanonical ATM activation in CSR.

Because we had identified a deficiency in the frequency of CSR in ATMIN$^{\Delta B/\Delta B}$-stimulated B cells and in immunized mice, we next addressed whether the accuracy of recombination was affected. To this end, we stimulated B cells in vitro to induce isotype switching to IgG1 and amplified Sγ1-Sμ junctions (Figure S2N). The fidelity of repair was comparable between ATMIN$^{F/F}$ and ATMIN$^{\Delta B/\Delta B}$ B cells because the frequency and the length of microhomology at the switch junction were similar between both genotypes (Figures S2O and S2P). We conclude that whereas ATMIN$^{\Delta B/\Delta B}$ cells show reduced efficiency of CSR, the accuracy of recombination is intact, as is the case in ATM$^{-/-}$ B cells (Reina-San-Martin et al., 2004).

SHM is a further mechanism used to generate antibody diversity, which is also initiated by AID. However, the repair of these lesions is thought to occur via MMR or BER and is ATM independent, supported by the finding that it occurs normally in ATM-deficient mouse mutants (Reina-San-Martin et al., 2004). Although SHM is not greatly disturbed in PMS2 or MLH1 deficiencies, ATMIN has been reported to affect MLH1-dependent MMR (McNees et al., 2005), and therefore, we investigated whether SHM could be affected in ATMIN$^{\Delta B/\Delta B}$ mice. We sorted B cells that had undergone SHM (B220⁺PNA⁺) from Peyer's Patches of aged mice (about 10-month-old mice were used to allow for accumulation of mutations) and sequenced the J$_H$4-C$_H$ intron of the Igh locus (as depicted in Figure S2N). By identifying 285 and 205 mutations within the J$_H$4-C$_H$ intron from ATMIN$^{F/F}$ and ATMIN$^{\Delta B/\Delta B}$ mice, respectively, we established that SHM can accumulate normally in ATMIN$^{\Delta B/\Delta B}$ mice with the observed frequency of mutations being comparable to those generated in ATMIN$^{F/F}$ mice (Figure S3A). Furthermore, the mutation load and the distribution of mutations identified in 59 and 50 clones for ATMIN$^{F/F}$ and ATMIN$^{\Delta B/\Delta B}$ mice, respectively, were largely unchanged (Figures S3B and S3C). These data argue against a function of ATMIN in SHM.

ATM Signaling in B Cells Requires ATMIN

We have previously shown that ATMIN is required for ATM activation in MEFs after treatment with agents that induce changes in chromatin structure (such as chloroquine and osmotic stress), but not after the generation of DNA DSBs by IR (Kanu and Behrens, 2007). Therefore, we wanted to determine whether ATMIN is also required for ATM activation under these conditions in B cells. We, therefore, purified B cells from spleens of control ATMIN$^{F/F}$ and ATMIN$^{\Delta B/\Delta B}$ mice, treated with IR (0.8 Gy) or osmotic stress (135 mOsm NaCl) and assessed ATM activation. ATM was activated efficiently by IR in both ATMIN$^{F/F}$ and ATMIN$^{\Delta B/\Delta B}$ B cells, as revealed by phosphorylation of the ATM substrate KAP1 at S824. However, ATM activation was dramatically reduced following osmotic stress in ATMIN$^{\Delta B/\Delta B}$ cells (Figure 3A). The total levels of ATM and KAP1 proteins were unchanged in ATMIN$^{\Delta B/\Delta B}$ B cells as compared to ATMIN$^{F/F}$ B cells. The survival of ATMIN-deficient B cells is not impaired in response to IR (Figure S3D), in line with our observation that ATM signaling in response to DSBs occurs normally.

During CSR presumably only a small number of DNA DSBs are generated. Although ATMIN was dispensable for ATM signaling by higher doses of IR, it was conceivable that ATMIN may be required for ATM signaling triggered by a small number of DSBs similar to what occurs during CSR (Figure 3B). Therefore, we treated B cells with 0.2 Gy IR (a dose that should only induce an average of 7.5 DSBs per cell) and found that ATM activation, as noted by phosphorylation of KAP1, was intact in ATMIN$^{\Delta B/\Delta B}$ B cells. Notably, ATM mRNA was increased in ATMIN$^{\Delta B/\Delta B}$ B cells compared with ATMIN$^{F/F}$ B cells (Figure 3C), and ATM protein was not reduced (Figure 3A).

To address whether ATMIN is required for ATM activation in cells undergoing CSR, we stained activated B cells treated with LPS/IL4 for P-ATM and γH2AX (Figure 3D). The localization of activated ATM to sites of DNA damage marked by γH2AX was less efficient upon loss of ATMIN (Figure 3E), providing additional evidence supporting a role for ATMIN in ATM function.
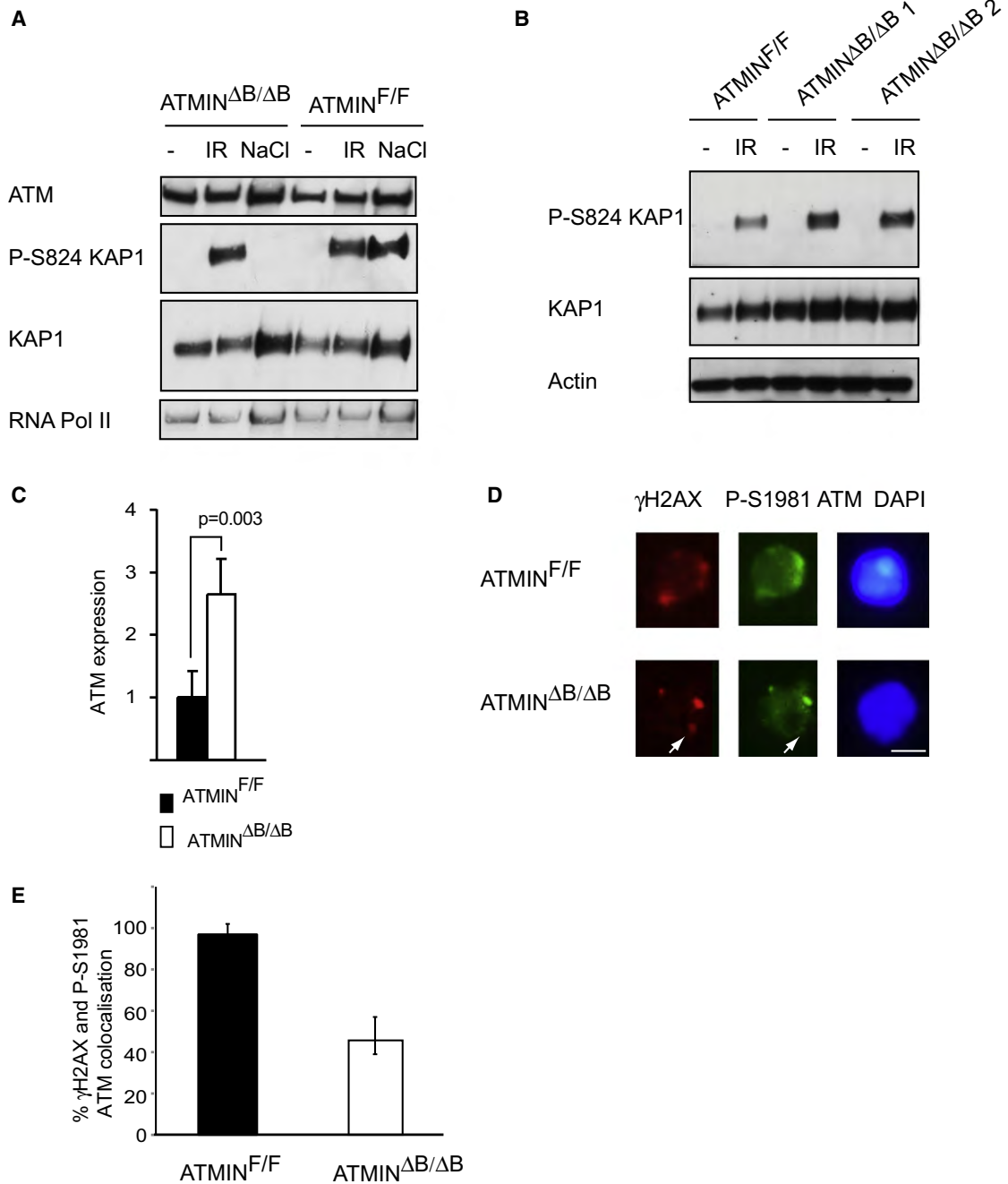
Figure 3. ATMIN Is Required for ATM Signaling in B Cells

(A) Purified B lymphocytes from ATMIN$^{F/F}$ and ATMIN$^{\Delta B/\Delta B}$ mice were untreated, treated with 0.8 Gy IR followed with 30 min incubation at 37°C, or treated with osmotic stress (50 mM NaCl = 135 mOsm) for 1 hr at 37°C. Cells were then lysed, proteins were resolved on a 3%–8% SDS-PAGE gel, and then transferred to a nitrocellulose membrane. The membrane was probed with the indicated antibodies.

(B) Purified B lymphocytes from ATMIN$^{F/F}$ and ATMIN$^{\Delta B/\Delta B}$ mice were either left untreated or treated with 0.2 Gy IR followed with 20 min incubation at 37°C. Cells were then lysed, proteins were resolved on a 3%–8% SDS-PAGE gel and then transferred to a nitrocellulose membrane. The membrane was probed with the indicated antibodies.

(C) Quantitative RT-PCR for ATM was performed on mRNA from ATMIN$^{F/F}$ and ATMIN$^{\Delta B/\Delta B}$ B lymphocytes. Levels of ATM mRNA were normalized to actin.

(D) Purified B lymphocytes from ATMIN$^{F/F}$ and ATMIN$^{\Delta B/\Delta B}$ mice cultured with LPS/IL4 for 2 days following which cells were stained for P-S1987 ATM, γH2AX (P-S139), and DAPI. Arrows indicate regions stained positive for γH2AX but negative for P-S1981 ATM. Scale bar, 5 μm. The quantification of 100 cells/treatment is shown in (E). Data are presented as mean and SD. Statistical analyses were calculated by a Student's t test with two-tailed distribution. p values are indicated. See also Figure S3.
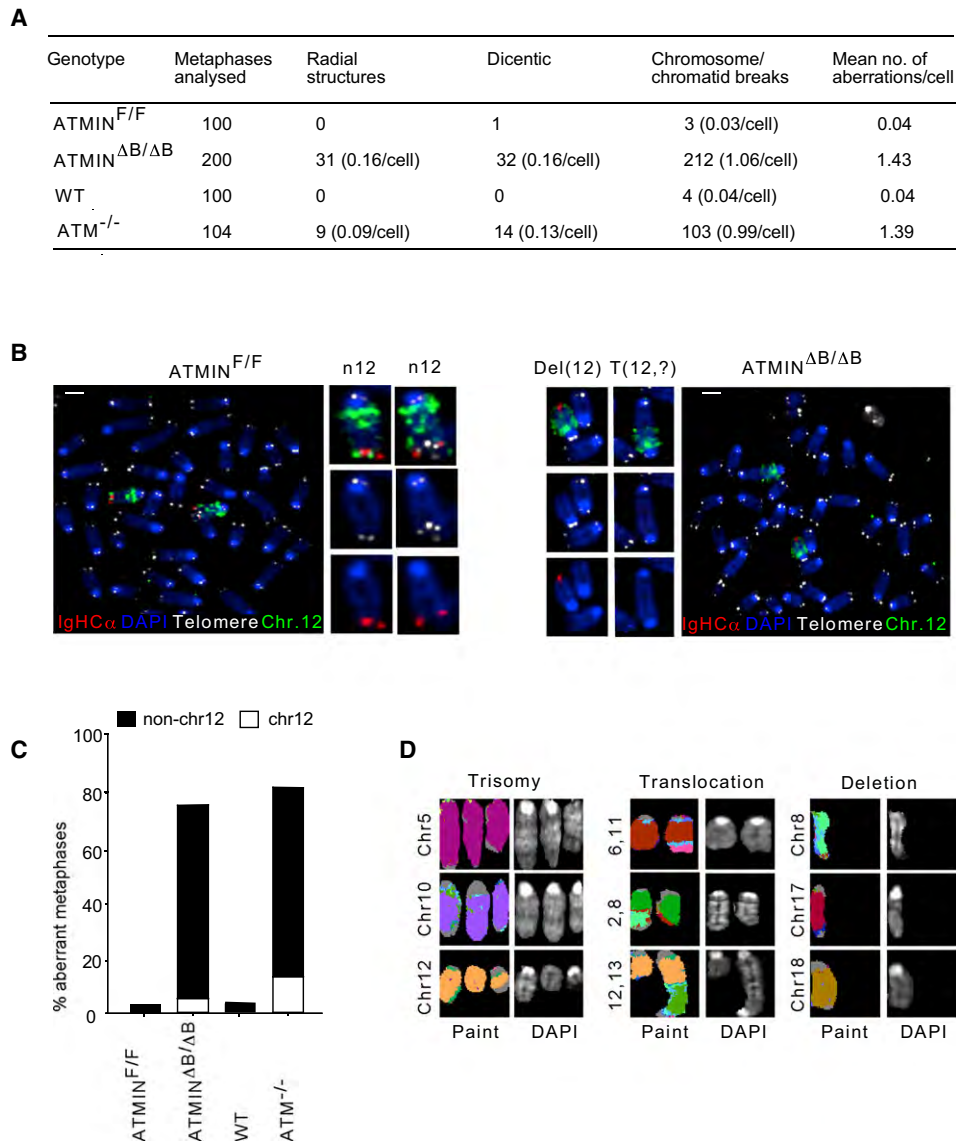
A

Genotype	Metaphases analysed	Radial structures	Dicentic	Chromosome/ chromatid breaks	Mean no. of aberrations/cell
ATMIN$^{F/F}$	100	0	1	3 (0.03/cell)	0.04
ATMIN$^{\Delta B/\Delta B}$	200	31 (0.16/cell)	32 (0.16/cell)	212 (1.06/cell)	1.43
WT	100	0	0	4 (0.04/cell)	0.04
ATM$^{-/-}$	104	9 (0.09/cell)	14 (0.13/cell)	103 (0.99/cell)	1.39

B

C

D

Figure 4. Loss of ATMIN Leads to Genomic Instability in B Cells

(A–C) (A) Metaphases from ATMIN$^{\Delta B/\Delta B}$ and ATM$^{-/-}$ B cells stimulated with LPS/IL4 form radial structures, dicentric chromosomes, and chromosome/chromatid breaks and also show instability of chromosome 12, whereas WT and ATMIN$^{F/F}$ control cells (n = 2 mice/genotype) do not display such abnormalities significantly (B and C). Deletions and translocations were observed within chromosome 12 (that carries the *Igh* locus) in ATMIN$^{\Delta B/\Delta B}$ but not ATMIN$^{F/F}$ metaphase cells stimulated with LPS/IL4 to induce CSR (identified using a painting probe for chromosome 12, a telomere probe, a BAC probe for *Igh*, and DAPI). Of 62 ATMIN$^{\Delta B/\Delta B}$ metaphases that showed aberrations within chromosome 12, 4 had putative *Igh* aberrations (positive for *IghCα* probe and negative for telomere probe), and 27 showed non-*Igh* aberrations (negative for both *IghCα* and telomere probes). In ATM$^{-/-}$ B cells, putative *Igh* aberrations occurred in 2 of 39 metaphases compared to 13 of 39 non-*Igh* aberrations. Scale bar, 2 μm.

(D) Using M-FISH, genomic instability represented by duplications, translocations, and deletions was observed in ATMIN$^{\Delta B/\Delta B}$ metaphase cells stimulated with LPS/IL4 to induce CSR but not in ATMIN$^{F/F}$ control cells (n = 4 per genotype for ATMIN$^{F/F}$ and ATMIN$^{\Delta B/\Delta B}$, n = 4 per genotype for WT and ATM$^{-/-}$).
See also Figure S4.

ATMIN Is Required to Maintain Genomic Stability

Because ATM function is required to suppress chromosomal translocations, we next asked whether ATMIN is required to suppress genomic instability. For this purpose we arrested ATMIN$^{F/F}$ and ATMIN$^{\Delta B/\Delta B}$ cells in metaphase following CSR and stained with a telomere probe, *Igh* probe (containing Cδ-Cα of the *Igh* locus), and a painting probe for chromosome 12 (that carries the *Igh* locus) combined with DAPI. We observed fusions, translocations, and deletions both within chromosome 12 and within other chromosomes in ATMIN$^{\Delta B/\Delta B}$ B cells compared with ATMIN$^{F/F}$ B cells (Figures 4A and 4B). A comparison of the instability of ATMIN$^{\Delta B/\Delta B}$ B cells with ATM$^{-/-}$ B cells revealed that deletion of either gene resulted in the formation of radial structures, dicentric chromosomes, and chromosome/chromatid breaks (Figure 4A; Figure S4A), with comparable frequencies. Therefore, similar to ATM, ATMIN is required to

maintain genomic stability of B cells. Instability was also observed in chromosomes other than chromosome 12, suggesting that ATMIN is required for maintaining global genomic stability of B cells (Figures 4B and 4C). In order to determine which chromosomes were involved in the instability that was not associated with chromosome 12, we performed multiplex-fluorescence in situ hybridization (M-FISH) and found a number of chromosomes to be duplicated (trisomy), translocated, and deleted. Examples of each form of instability are shown in Figure 4D (the complete M-FISH profiles of ten ATMIN$^{\Delta B/\Delta B}$, ten ATM$^{-/-}$, six ATMIN$^{F/F}$, and six WT B are shown in Figures S4B–S4E).

It has recently been demonstrated that peripheral B cells attempt secondary V(D)J recombination and that activated NHEJ-deficient splenic B cells accumulate V(D)J recombination-associated breaks at the *Igl* locus (Wang et al., 2009). To assess the stability of the *Igl* locus in basal conditions and following CSR, we performed 3D FISH on ATMIN$^{\Delta B/\Delta B}$ and ATM$^{-/-}$ cells along with their respective controls using 3′ and 5′ *Igl* probes (Figure 5A). Using this approach, we found that both ATMIN and ATM are required to maintain stability of the *Igl* locus in peripheral B cells that undergo secondary V(D)J recombination. Normally the 5′ and 3′ *Igl* probes colocalize on both alleles (Figure 5B). However, following the induction of CSR, RAG1/2 induces peripheral B cells to undergo secondary V(D)J recombination of *Igl*, and the repair of these breaks appears to occur with decreased efficiency in the absence of ATMIN or ATM, leading to increased incidence of broken *Igl* loci compared to controls (Figure 5C; Figure S5). These data further demonstrate the requirement for ATMIN in maintaining the global genomic stability of B cells.

Deletion of ATMIN in B Cells Results in B Cell Lymphoma

DSBs are formed in *Ig* loci during antibody gene diversification reactions, and a defect in the repair of these breaks tends to lead to oncogenic *Ig* translocations in several mouse models for DNA repair genes (Callen et al., 2007a, 2009; Celeste et al., 2002; Difilippantonio et al., 2000, 2002; Difilippantonio et al., 2005; Reina-San-Martin et al., 2005). However, such translocations have often only been observed in cultured cells, and loss-of-function mouse models for many repair genes have not been reported to generate B cell lymphomas in vivo. Indeed, the humanized mouse model for NBS1 (hNbs1$^{657\Delta5}$) develops B cell and thymic lymphomas only in a p53$^{-/-}$ background (Reina-San-Martin et al., 2005). In contrast, approximately 40% of ATMIN$^{\Delta B/\Delta B}$ mice develop B cell lymphomas at around 6 months of age (Figure 6A), as characterized by a dramatic increase in the size of the spleen in comparison to that of ATMIN$^{F/F}$ littermates (Figure 6B).

H&E of the spleens from ATMIN$^{\Delta B/\Delta B}$ mice with B cell lymphomas demonstrated a disorganized structure, with the germinal centers (GCs) being largely indistinguishable from the red pulp (RP) (Figure 6C). The development of lymphoma was confirmed by the infiltration of B cells to multiple organs including the lungs, as shown by B220 staining (Figure 6D). Furthermore, the tumor cell infiltrates to the liver were positive for B220 but negative for CD3 and Mac2, hence confirming that the tumors were of a B cell origin and not of a T cell or macrophage origin (Figure S6). The infiltration of tumor cells was particularly apparent around the blood vessels, as indicated in the liver (Figure S6).
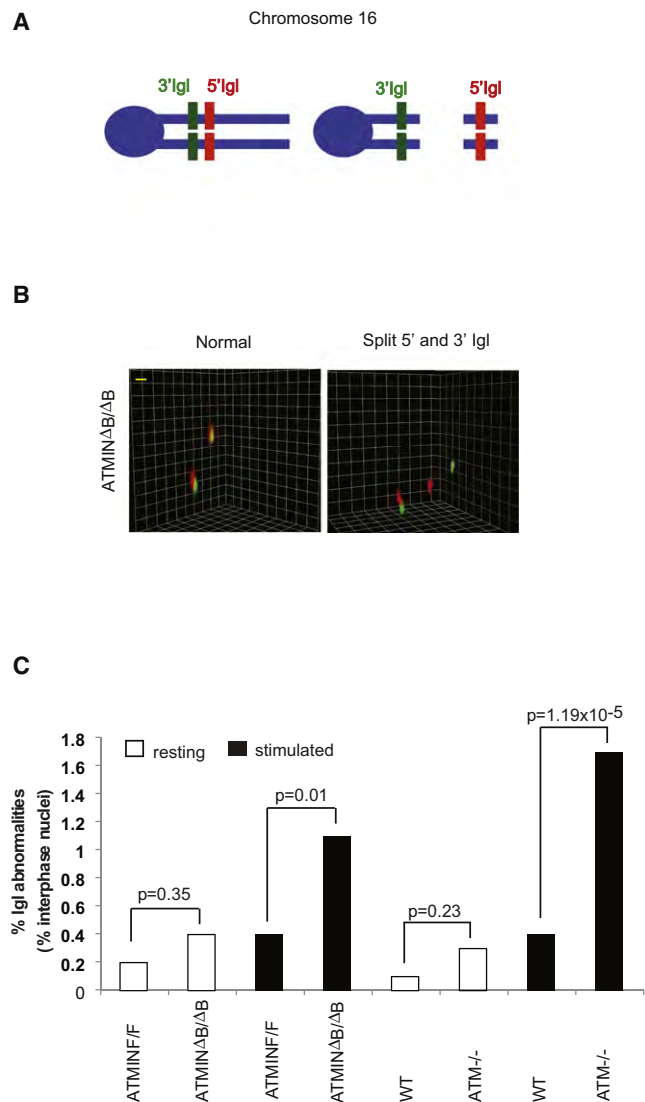
Figure 5. ATMIN Is Required to Repair RAG1/2-Induced Breaks in Peripheral B Cells
(A) Using a painting probe for chromosome 16, 3′*Igl* probe in green and 5′*Igl* probe in red, the repair of RAG1/2-induced breaks was measured.
(B) 3D FISH was performed on unstimulated and 3 day LPS-stimulated ATMIN$^{\Delta B/\Delta B}$ and ATM$^{-/-}$ B cells along with their controls using probes located in the 5′ and 3′ of the *Igl* locus. Scale bar, 1 μm.
(C) Quantification of (B). p values were calculated using the chi-square test. See also Figure S5.

To determine the expression profile of ATMIN in the spleen, we performed in situ hybridization. In 6-week-old ATMIN$^{F/F}$ control mice, *atmin* mRNA expression was confined mostly to the GCs (Figure 6E). *atmin* mRNA was absent in ATMIN$^{\Delta B/\Delta B}$ spleens, indicating that B cells express high levels of *atmin* mRNA (and also serving as a negative control for the specificity of the in situ hybridization, Figure 6E). Spleens from ATMIN$^{\Delta B/\Delta B}$ mice with B cell lymphoma showed no *atmin* expression, hence indicating that the lymphoma originated from ATMIN$^{\Delta B/\Delta B}$ cells.

To assess the tumorigenic potential of B cells from ATMIN$^{\Delta B/\Delta B}$ mice with B cell lymphomas, we engrafted total splenocytes into
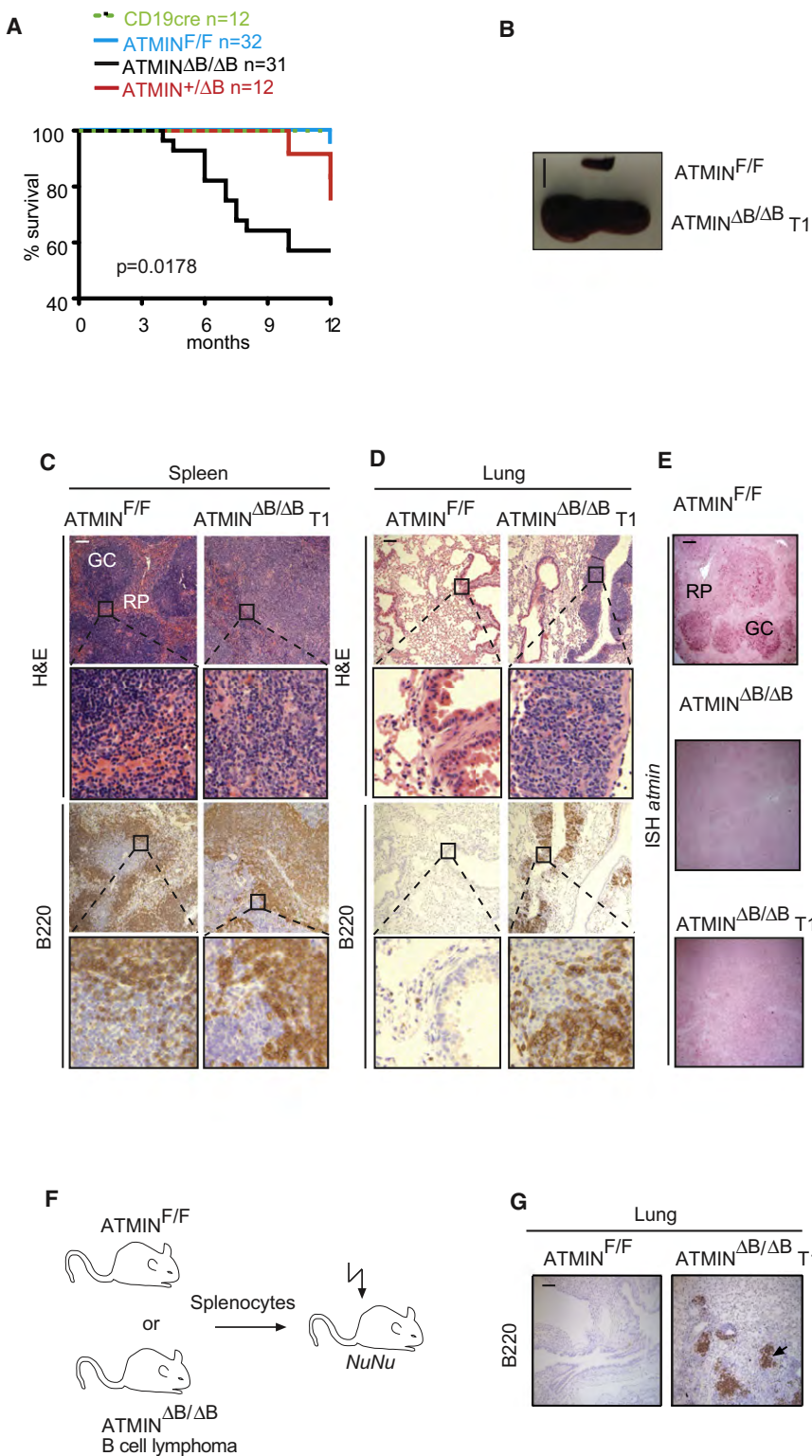
Figure 6. ATMIN Is Required to Suppress B Cell Lymphoma

(A) ATMIN$^{\Delta B/\Delta B}$ mice develop B cell lymphoma at a mean age of 6.5 months. Log rank (Mantel-Cox) test was used to compare ATMIN$^{F/F}$ to ATMIN$^{\Delta B/\Delta B}$ (p = 0.0178).

(B) Macroscopic analysis of spleens from ATMIN$^{\Delta B/\Delta B}$ mice with B cell lymphoma (ATMIN$^{\Delta B/\Delta B}$ T1) compared with age-matched ATMIN$^{F/F}$ mouse (scale bar, 1 cm).

(C) H&E and B220 staining of the spleen from ATMIN$^{F/F}$ and ATMIN$^{\Delta B/\Delta B}$ T1 mice revealed a loss of discrete GCs and RP regions, in the latter case. Scale bar, 100 μm.

(D) H&E and B220 staining of the lungs displayed an infiltration of B220^{+} but also B220^{-} cells in ATMIN$^{\Delta B/\Delta B}$ T1. Scale bar, 100 μm. The dashed lines and boxes in (C) and (D) indicate regions that are represented in the panels below at higher magnification.

(E) In situ hybridization for *atmin* indicates its localization mainly to the GCs of ATMIN$^{F/F}$ spleens and that expression is lost in spleens from ATMIN$^{\Delta B/\Delta B}$ and ATMIN$^{\Delta B/\Delta B}$ T1 mice. Scale bar, 100 μm.

(F) ATMIN$^{\Delta B/\Delta B}$ lymphomas are transplantable. Schematic representation for the engraftment of ATMIN$^{F/F}$ or ATMIN$^{\Delta B/\Delta B}$ B cell lymphoma into sublethally irradiated *NuNu* mice.

(G) Splenocytes from ATMIN$^{\Delta B/\Delta B}$ B cell lymphomas but not splenocytes from ATMIN$^{F/F}$ are transplantable as indicated by infiltration of B cells to the lungs (indicated by arrow). ATMIN$^{\Delta B/\Delta B}$ T1–T4 were transplanted individually into three host *NuNu* mice. ATMIN$^{\Delta B/\Delta B}$ T1 engraftment is indicated in the figure as a representative result. Scale bar, 100 μm.

See also Figure S6.

these moribund mice the spleens were slightly increased in size, and lymphoma cells were found in multiple tissues, including the lungs and liver (Figure 6G; data not shown). Hence, transplantation of ATMIN$^{\Delta B/\Delta B}$ splenocytes causes lymphoid tumor development in host animals, confirming their tumorigenic potential in vivo. Thus, deletion of ATMIN in B cells leads to the formation of B cell lymphoma.

ATMIN$^{\Delta B/\Delta B}$ B Cell Lymphomas Are Phenotypically Diverse and Carry Global Genomic Instability

If ATMIN is required for maintaining global genomic instability, this would imply that the B cell lymphomas that develop due to loss of ATMIN should be phenotypically diverse. FACS analyses of spleens from ATMIN$^{\Delta B/\Delta B}$ mice with B cell lymphomas revealed that this was indeed the case (Figure 7A; Figure S7). Furthermore, M-FISH analyses demonstrated that tumor cells harbored genomic aberrations of

sublethally irradiated *NuNu* mice (Figure 6F). Around 2-4 months post-engraftment, recipient mice receiving cells from the spleens of moribund ATMIN$^{\Delta B/\Delta B}$ mice, but not those receiving ATMIN$^{F/F}$ control splenocytes, appeared moribund and were culled. In
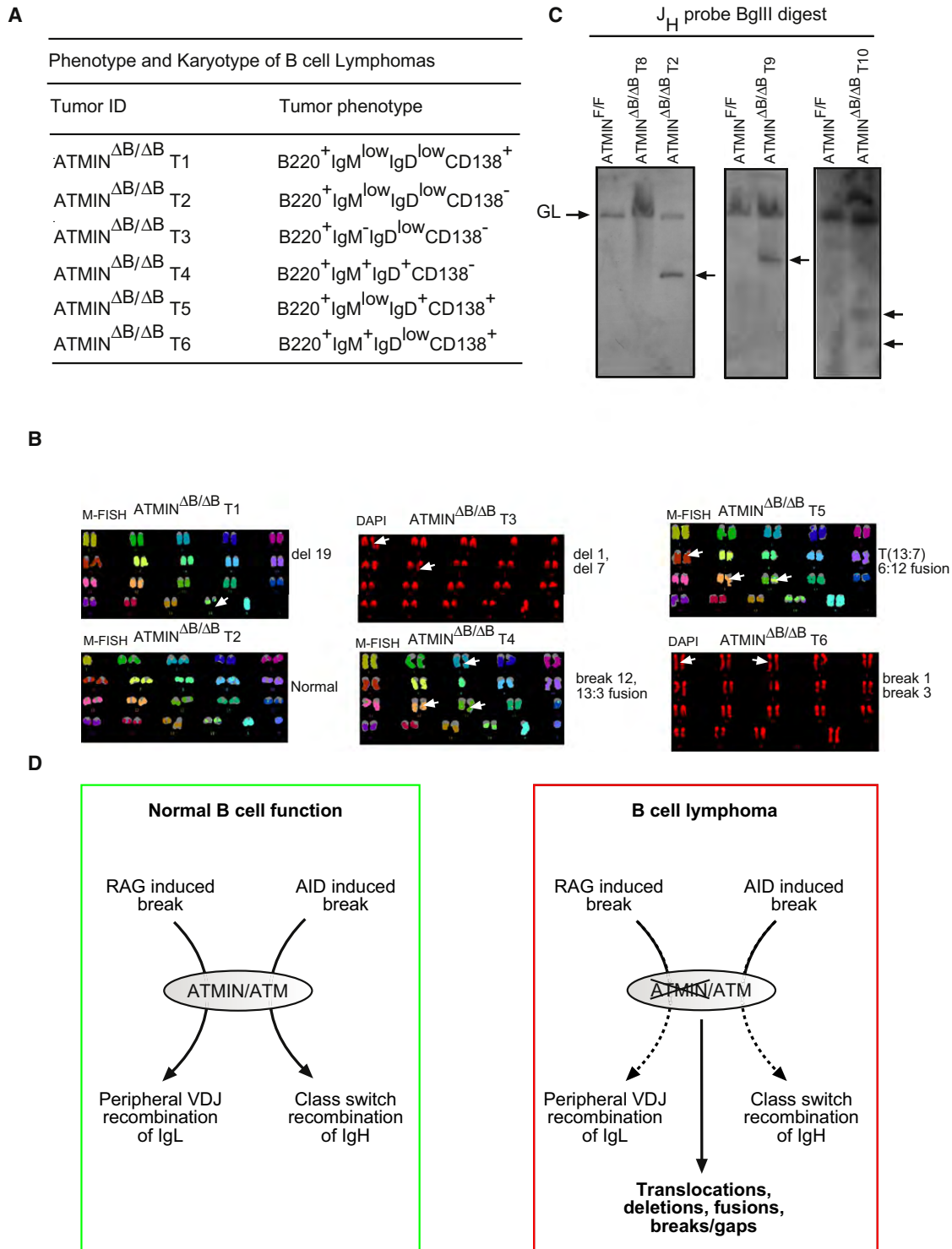
A

Phenotype and Karyotype of B cell Lymphomas

Tumor ID	Tumor phenotype
ATMIN$^{\Delta B/\Delta B}$ T1	B220$^+$IgM^{low}IgD^{low}CD138$^+$
ATMIN$^{\Delta B/\Delta B}$ T2	B220$^+$IgM^{low}IgD^{low}CD138$^-$
ATMIN$^{\Delta B/\Delta B}$ T3	B220$^+$IgM$^-$IgD^{low}CD138$^-$
ATMIN$^{\Delta B/\Delta B}$ T4	B220$^+$IgM$^+$IgD$^+$CD138$^-$
ATMIN$^{\Delta B/\Delta B}$ T5	B220$^+$IgM^{low}IgD$^+$CD138$^+$
ATMIN$^{\Delta B/\Delta B}$ T6	B220$^+$IgM$^+$IgD^{low}CD138$^+$

C

B

D

Figure 7. ATMIN$^{\Delta B/\Delta B}$ Lymphomas Arise Due to Genomic Instability

(A) Phenotypic FACS analysis of lymphomas indicates them to be heterogeneous.

(B) Cells from ATMIN$^{\Delta B/\Delta B}$ mice with B cell lymphomas (ATMIN$^{\Delta B/\Delta B}$ T1–T6) were analyzed by M-FISH and DAPI staining to identify cytogenetic abnormalities. del, deletions; break, chromosome/chromatid breaks/gaps; fusion, dicentric chromosomes; T, translocations. At least five metaphases were analyzed.

(C) Southern blot for JH region of the *Igh* locus using DNA isolated from ATMIN$^{\Delta B/\Delta B}$ B cell lymphomas. The arrows on the right of each panel indicate bands specific for the rearranged *Igh* locus.

(D) Model for the role of ATMIN in suppressing translocations.

See also Figure S7.

immunoglobulin and nonimmunoglobulin chromosomes (Figure 7B). Southern blotting for the JH region of the *Igh* locus indicated these B cell lymphomas to be mostly monoclonal (Figure 7C).

DISCUSSION

Using a mouse model lacking ATMIN function in B cells, we have shown that ATMIN is required during the maturation of B cells and for the repair of breaks that are generated during CSR. Furthermore, ATMIN$^{\Delta B/\Delta B}$ mice develop B cell lymphomas, and ATMIN$^{\Delta B/\Delta B}$ B cells are characterized by global genomic instability.

Similar Phenotypes of ATM and ATMIN Deficiency in B Cells

The ATMIN$^{\Delta B/\Delta B}$ phenotype shares several similarities with ATM deficiency. First, like ATM, ATMIN is required during the early maturation of B cells; however, both ATMIN$^{\Delta B/\Delta B}$ mice and ATM$^{-/-}$ mice have normal numbers of mature splenic B cells (Figure 1; Figures S1F–S1J) (Xu et al., 1996). Second, both ATMIN and ATM are required for efficient CSR (Figure 2; Figures S2A–S2M), but the fidelity of repair at switch junctions is unaffected in both ATM$^{-/-}$ and ATMIN$^{\Delta B/\Delta B}$ B cells (Figures S2O and S2P) (Reina-San-Martin et al., 2004). Third, the efficiency of generating antibody diversity by SHM of the variable region of the *Igh* locus is unaffected by both ATMIN and ATM deficiency (Figures S3A–S3C) (Reina-San-Martin et al., 2004). Finally, the genomic instability observed in ATMIN$^{\Delta B/\Delta B}$ B cells is similar both quantitatively and qualitatively to that observed in ATM$^{-/-}$ cells (Figures 4, 5, Figures S4B–S4E, and S5). Taken together, the similarities shared between ATMIN$^{\Delta B/\Delta B}$ mice and ATM$^{-/-}$ mice, together with the reduced ATM activity in response to hypotonic stress, indicate that ATMIN has physiological relevance for ATM function in B cells. However, it is worth noting that ATM-independent functions of ATMIN may well contribute to the phenotype in ATMIN$^{\Delta B/\Delta B}$ mutant mice.

Functional Significance of DSB-Independent ATM Activation

The ATM-signaling pathway can be triggered by different stimuli. The best-characterized pathway of ATM activation is the response to DSBs, experimentally induced by IR and many other agents such as topoisomerase inhibitors. But in addition to DNA breaks, ATM activation is also triggered by hypotonic stress that induces chromatin conformation changes (Bakkenist and Kastan, 2003). NBS1 null B cells are defective in ATM signaling after IR, but ATM activation in response to hypotonic stress is intact (Difilippantonio et al., 2005). The requirement of ATMIN for ATM activity appears to be complementary to NBS1. The activation of ATM after hypotonic stress is mediated by ATMIN, whereas ATM activation following IR is normal in ATMIN$^{\Delta B/\Delta B}$ cells (Figures 3A and 3B). Thus, ATMIN deficiency inactivates the arm of ATM signaling triggered by hypotonic stress in B cells.

Although MRN-dependent ATM activation is triggered by DSBs, at present, the molecular signal triggering ATMIN-dependent ATM activation is not known. ATM signaling induced by hypotonic stress is defective in both ATMIN-deficient murine MEFs and B cells, as well as in HEK293T cells transfected with sh-ATMIN knockdown constructs (Kanu and Behrens, 2007). Thus, the pathway of ATM activation mimicked by hypotonic stress is unlikely to be B cell specific but rather a second generic mode of ATM activation. Hypotonic stress and chloroquine are believed to act by altering chromatin structure (Bakkenist and Kastan, 2003), and the identification of the chromatin-based stimulus of ATMIN-dependent ATM activation will be required for a complete understanding of ATMIN and ATM functions.

Nonredundant Biological Functions of ATMIN and NBS1

Although both ATMIN$^{\Delta B/\Delta B}$ and NBS1$^{\Delta B/\Delta B}$ B cells have a 50% defect in CSR, ATM$^{-/-}$ B cells have a more dramatic defect (around 70%–80% reduction) (Figure 2D) (Kracker et al., 2005; Lumsden et al., 2004; Reina-San-Martin et al., 2004, 2005). The inhibition of ATM in ATMIN$^{\Delta B/\Delta B}$ cultures reduces the amount of CSR to levels comparative to ATM$^{-/-}$ cultures, i.e., the effects of ATM and ATMIN deficiencies are not additive. This is in agreement with the notion that ATMIN functions at least in part through regulation of ATM signaling during CSR. Their nonredundant biological functions indicate that for efficient ATM-dependent CSR to occur, both ATMIN and NBS1 are required. This implies that canonical ATM activation and noncanonical ATM activation are both essential during CSR. The nonoverlapping functions of ATMIN and NBS1 might reflect functions at different stages and/or different aspects of CSR.

A further difference between ATMIN$^{\Delta B/\Delta B}$ mice and a mouse model for patients with NBS, in which a 5 bp hypomorphic allele is expressed in an NBS null background (hNbs1$^{657\Delta5}$), is that whereas both models display genomic instability, ATMIN$^{\Delta B/\Delta B}$ mice develop B cell lymphomas, but hNbs1$^{657\Delta5}$ mice only develop B and T cell lymphomas in a p53$^{-/-}$ background (Difilippantonio et al., 2005). T cell thymomas are the main cause of lethality of ATM$^{-/-}$ mice and occur due to defective TCR rearrangement (Barlow et al., 1996; Liyanage et al., 2000; Matei et al., 2007; Xu et al., 1996). In contrast, deletion of NBS1 in T cells does not lead to the formation of thymomas (Saidi et al., 2010). Our unpublished data indicate that deletion of ATMIN using a *Vav*-cre transgene that deletes from the hematopoietic stem cell onward does lead to the development of T cell lymphomas, albeit with low penetrance. However, whether this is due to defective TCR rearrangement remains to be shown. Hence, whereas both ATMIN and NBS1 are required to maintain genomic stability, absence of ATMIN and ATM in immune cells leads to the generation of lymphomas, whereas in the case of NBS1 deletion, a further oncogenic hit appears to be required.

ATMIN Function in B Cell Lymphoma

We show that the absence of ATMIN in B cells leads to the development of B cell lymphomas (Figures 6 and 7; Figures S6 and S7). ATMIN$^{\Delta B/\Delta B}$ mice reveal a role for ATMIN in the repair of both RAG1/2 and AID-induced breaks in peripheral B cells (Figures 4 and 5). In the absence of ATMIN, breaks generated by peripheral V(D)J rearrangement and CSR are inappropriately repaired, resulting in translocations, deletions, fusions, and chromatid/chromosome breaks and gaps, ultimately leading to B cell lymphoma.

Genomic instability that arises in ATM$^{-/-}$ B cells has been reported to result from RAG1/2-dependent *Igh*-associated breaks that can persist throughout B cell development (Callen et al., 2007b). We are using CD19-cre to delete ATMIN, which mediates deletion from the pro-B cell stage, when *Igh* rearrangement should be largely completed. Thus, we hypothesize that the genomic instability in ATMIN$^{\Delta B/\Delta B}$ B cells is mainly a result of AID-induced breaks that are not efficiently repaired. However, we have also observed that ATMIN is required for repair of breaks caused by peripheral V(D)J recombination induced by RAG1/2 (Figure 5). Thus, *Igl* breaks may persist in ATMIN-deficient B cells and contribute to genomic instability.

The ATMIN$^{\Delta B/\Delta B}$ lymphomas are heterogeneous, as is the case with some models of B cell lymphoma, including transgenic mice overexpressing AID (Figure 7; Figure S7) (Robbiani et al., 2009). Furthermore, genomic instability was found to occur on chromosomes other than those carrying immunoglobulin loci. This raises the possibility that ATMIN might function as a tumor suppressor also in nonlymphoid tissues.

It is puzzling that ATMIN$^{\Delta B/\Delta B}$ mice develop B cell lymphomas, whereas ATM$^{-/-}$ mice do not. However, homozygous mice harboring an in-frame deletion of ATM corresponding to the human 7636 del9 mutation show an increased susceptibility to developing tumors, including B cell lymphoma (Spring et al., 2001, 2002). Also, A-T patients exhibit a predisposition to the development of a wide range of lymphoid tumors of both T and B cell origin (Stankovic et al., 2002). Thus, it appears that the nature of the ATM mutation determines the tumor spectrum.

ATM activity is believed to have two main functions in the suppression of CSR-associated chromosomal translocations. First, ATM has been suggested to facilitate CSR by stabilizing the synapsis of distal switch regions, and therefore, the absence of ATM may increase the frequency of abnormal translocations (Callen et al., 2007a). Second, ATM signaling has been shown to constitute a barrier against oncogenic transformation. Increased expression of oncogenes as a result of aberrant translocations can lead to oncogenic stress and induces an ATM-dependent DNA-damage response (Bartkova et al., 2005, 2006; Mallette et al., 2007). Thus, the ATM-dependent checkpoint may antagonize lymphoma development by eliminating cells before or after they suffer an oncogenic translocation. The relative contribution of ATMIN and NBS1 for ATM function in tumor suppression is not known.

Interestingly, analysis of *atmin* expression using published data describing transcriptional profiling of human patients with B cell acute lymphoblastic leukemia (B-ALL) revealed that the expression of *atmin* was reduced in B-ALL as compared to normal pre-B and immature B cells (Maia et al., 2005). Thus, reduced *atmin* expression may also contribute to the development of human B cell lymphomas.

This study has revealed an important function for ATMIN in B cells. We have shown that ATMIN is required to prevent chromosomal instability in B cell lymphoma. A better understanding of chromosomal instability in lymphoid cancers and how tumor-suppressive pathways normally limit the frequency of these aberrant recombination events will be crucial for the development of more efficient chemotherapeutics (Bunting et al., 2010; Nussenzweig and Nussenzweig, 2010).

EXPERIMENTAL PROCEDURES

Mice

Mice with a targeted mutation of the *atmin* gene were generated by insertion of lox P sequences upstream and downstream of exon 4 of *atmin* (ATMIN^F) in embryonic stem (ES) cells, injection of ATMIN$^{WT/F}$ into blastocysts, and mating of the resulting chimera. For cre-mediated deletion of *atmin* in B lymphocytes, ATMIN$^{F/F}$ mice were crossed with heterozygous CD19-cre mice and were designated ATMIN$^{\Delta B/\Delta B}$. ATM mice were bred as ATM$^{+/-}$ and have been described previously (Barlow et al., 1996). Immunocompromised ICRF *NuNu* mice were maintained in-house. Unless otherwise stated, all mice were used at 6–12 weeks of age. CD19-cre deletion efficiency and genotyping of mice were determined using a PCR-based assay using primers specific for the floxed exon 4, deleted exon 4, and WT *atmin* alleles as well as primers for CD19-cre and WT *CD19* alleles using the primers:

> Lox6133F 5′-TCAGCATCTTCTCCAGAGAGACAG-3′,
> Lox6617R 5′-CACATGTGTACAGCACATTCATTG-3′,
> Lox10252R 5′-CTCAGGGTACACATACTATGCTTGC-3′
> CD1902 5′-CCACAGAGGGAGGCAATGTTGTGC-3′
> CD19.15R 5′-GTCCTTGAAAGGGGGGCCTCTTCTGGC-3′
> Cre19.2R 5′-ACGACCGGCAAACGGACAGAAGCA-3′

Animals were maintained and bred in the London Research Institute Biological Resources. All experimental procedures were approved by London Research Institute ethics committees and conform to the UK Home Office regulations.

Immunizations

Mice were immunized as described previously (Lumsden et al., 2004) with slight modifications. Briefly, mice were injected intraperitoneally with 100 μg TNP-KLH (Biosearch Technologies Inc.) in Imject Freunds Complete Adjuvant (FCA) (at a ratio of 1:1 [Thermo Scientific]), and serum was collected on day 0 before immunization and on days 7, 14, 21, and 39 after immunization. Mice were boosted in the same manner on day 40, and serum was collected on day 7. Total and antigen-specific serum immunoglobulins were assayed by ELISA.

Engraftment of B Cell Lymphomas

Splenocytes (8.5 × 10^6 cells in 100 μl) from four control ATMIN$^{F/F}$ mice and four ATMIN$^{\Delta B/\Delta B}$ mice with B cell lymphomas (T1–T4) were injected into the tail vein of sublethally irradiated (374 rad) *NuNu* recipients (three recipients per host sample). Around 2-4 months postinjection mice injected with ATMIN$^{\Delta B/\Delta B}$ T1–T4 splenocytes, but not ATMIN$^{F/F}$ splenocytes, became moribund and were culled.

Purification, In Vitro Activation, and Treatment of B Cells

Single-cell suspensions of B lymphocytes were generated from murine spleens by lysis of red blood cells using ammonium chloride (STEMCELL Technologies) and negative selection following incubation with biotin-conjugated antibodies (CD4, CD8, TCRβ, TCRγδ, CD49b, Mac1, Ter119 [BD PharMingen]) and then streptavidin-conjugated Dynabeads (Invitrogen). For in vitro activation, B lymphocytes were cultured at 1 × 10^6 cells/ml in RPMI 1640 medium (Invitrogen) supplemented with penicillin/streptomycin (Invitrogen), L-glutamine (Invitrogen), 10% FCS (Sigma), and 5 × 10^{-5} M β-mercaptoethanol (Sigma) with 15 μg/ml *Escherichia coli* lipopolysaccharide (LPS; Sigma) with or without 50 ng/ml IL4 (Sigma) and CD40L at 100ng/ml (R&D Systems). The ATM inhibitor Ku55993 (Hickson et al., 2004) (Merck) was used at 10 μM throughout the culture duration. IR experiments were performed using a Cs137 Gamma Irradiator for the indicated times. Hypotonic swelling was performed using 50 mM NaCl (135 mOsm) in 1% FBS/PBS supplemented with 0.45% glucose for 1 hr at 37°C as described previously (Difilippantonio et al., 2005). Cells were incubated for the indicated time points before FACS analysis, ELISA, or extraction of DNA, RNA, or protein.

SUPPLEMENTAL INFORMATION

Supplemental Information includes Supplemental Experimental Procedures and seven figures and can be found with this article online at doi:10.1016/j.ccr.2011.03.022.

REFERENCES

Bakkenist, C.J., and Kastan, M.B. (2003). DNA damage activates ATM through intermolecular autophosphorylation and dimer dissociation. Nature *421*, 499–506.

Barlow, C., Hirotsune, S., Paylor, R., Liyanage, M., Eckhaus, M., Collins, F., Shiloh, Y., Crawley, J.N., Ried, T., Tagle, D., and Wynshaw-Boris, A. (1996). Atm-deficient mice: a paradigm of ataxia telangiectasia. Cell *86*, 159–171.

Bartkova, J., Horejsi, Z., Koed, K., Kramer, A., Tort, F., Zieger, K., Guldberg, P., Sehested, M., Nesland, J.M., Lukas, C., et al. (2005). DNA damage response as a candidate anti-cancer barrier in early human tumorigenesis. Nature *434*, 864–870.

Bartkova, J., Rezaei, N., Liontos, M., Karakaidos, P., Kletsas, D., Issaeva, N., Vassiliou, L.V., Kolettas, E., Niforou, K., Zoumpourlis, V.C., et al. (2006). Oncogene-induced senescence is part of the tumorigenesis barrier imposed by DNA damage checkpoints. Nature *444*, 633–637.

Bunting, S.F., Callen, E., Wong, N., Chen, H.T., Polato, F., Gunn, A., Bothmer, A., Feldhahn, N., Fernandez-Capetillo, O., Cao, L., et al. (2010). 53BP1 inhibits homologous recombination in Brca1-deficient cells by blocking resection of DNA breaks. Cell *141*, 243–254.

Callen, E., Nussenzweig, M.C., and Nussenzweig, A. (2007a). Breaking down cell cycle checkpoints and DNA repair during antigen receptor gene assembly. Oncogene *26*, 7759–7764.

Callen, E., Jankovic, M., Difilippantonio, S., Daniel, J.A., Chen, H.T., Celeste, A., Pellegrini, M., McBride, K., Wangsa, D., Bredemeyer, A.L., et al. (2007b). ATM prevents the persistence and propagation of chromosome breaks in lymphocytes. Cell *130*, 63–75.

Callen, E., Jankovic, M., Wong, N., Zha, S., Chen, H.T., Difilippantonio, S., Di Virgilio, M., Heidkamp, G., Alt, F.W., Nussenzweig, A., and Nussenzweig, M. (2009). Essential role for DNA-PKcs in DNA double-strand break repair and apoptosis in ATM-deficient lymphocytes. Mol. Cell *34*, 285–297.

Camacho, E., Hernandez, L., Hernandez, S., Tort, F., Bellosillo, B., Bea, S., Bosch, F., Montserrat, E., Cardesa, A., Fernandez, P.L., and Campo, E. (2002). ATM gene inactivation in mantle cell lymphoma mainly occurs by truncating mutations and missense mutations involving the phosphatidylinositol-3 kinase domain and is associated with increasing numbers of chromosomal imbalances. Blood *99*, 238–244.

Celeste, A., Petersen, S., Romanienko, P.J., Fernandez-Capetillo, O., Chen, H.T., Sedelnikova, O.A., Reina-San-Martin, B., Coppola, V., Meffre, E., Difilippantonio, M.J., et al. (2002). Genomic instability in mice lacking histone H2AX. Science *296*, 922–927.

D'Amours, D., and Jackson, S.P. (2002). The Mre11 complex: at the crossroads of dna repair and checkpoint signalling. Nat. Rev. Mol. Cell Biol. *3*, 317–327.

Difilippantonio, M.J., Zhu, J., Chen, H.T., Meffre, E., Nussenzweig, M.C., Max, E.E., Ried, T., and Nussenzweig, A. (2000). DNA repair protein Ku80 suppresses chromosomal aberrations and malignant transformation. Nature *404*, 510–514.

Difilippantonio, M.J., Petersen, S., Chen, H.T., Johnson, R., Jasin, M., Kanaar, R., Ried, T., and Nussenzweig, A. (2002). Evidence for replicative repair of DNA double-strand breaks leading to oncogenic translocation and gene amplification. J. Exp. Med. *196*, 469–480.

Difilippantonio, S., Celeste, A., Fernandez-Capetillo, O., Chen, H.T., Reina San Martin, B., Van Laethem, F., Yang, Y.P., Petukhova, G.V., Eckhaus, M., Feigenbaum, L., et al. (2005). Role of Nbs1 in the activation of the Atm kinase revealed in humanized mouse models. Nat. Cell Biol. *7*, 675–685.

Fang, N.Y., Greiner, T.C., Weisenburger, D.D., Chan, W.C., Vose, J.M., Smith, L.M., Armitage, J.O., Mayer, R.A., Pike, B.L., Collins, F.S., and Hacia, J.G. (2003). Oligonucleotide microarrays demonstrate the highest frequency of ATM mutations in the mantle cell subtype of lymphoma. Proc. Natl. Acad. Sci. USA *100*, 5372–5377.

Haidar, M.A., Kantarjian, H., Manshouri, T., Chang, C.Y., O'Brien, S., Freireich, E., Keating, M., and Albitar, M. (2000). ATM gene deletion in patients with adult acute lymphoblastic leukemia. Cancer *88*, 1057–1062.

Hickson, I., Zhao, Y., Richardson, C.J., Green, S.J., Martin, N.M., Orr, A.I., Reaper, P.M., Jackson, S.P., Curtin, N.J., and Smith, G.C. (2004). Identification and characterization of a novel and specific inhibitor of the ataxia-telangiectasia mutated kinase ATM. Cancer Res. *64*, 9152–9159.

Kanu, N., and Behrens, A. (2007). ATMIN defines an NBS1-independent pathway of ATM signalling. EMBO J. *26*, 2933–2941.

Kanu, N., Penicud, K., Hristova, M., Wong, B., Irvine, E., Plattner, F., Raivich, G., and Behrens, A. (2010). The ATM cofactor ATMIN protects against oxidative stress and prevents accumulation of DNA damage in the ageing brain. J. Biol. Chem. *285*, 38534–38542.

Kracker, S., Bergmann, Y., Demuth, I., Frappart, P.O., Hildebrand, G., Christine, R., Wang, Z.Q., Sperling, K., Digweed, M., and Radbruch, A. (2005). Nibrin functions in Ig class-switch recombination. Proc. Natl. Acad. Sci. USA *102*, 1584–1589.

Lee, J.H., and Paull, T.T. (2004). Direct activation of the ATM protein kinase by the Mre11/Rad50/Nbs1 complex. Science *304*, 93–96.

Liyanage, M., Weaver, Z., Barlow, C., Coleman, A., Pankratz, D.G., Anderson, S., Wynshaw-Boris, A., and Ried, T. (2000). Abnormal rearrangement within the alpha/delta T-cell receptor locus in lymphomas from Atm-deficient mice. Blood *96*, 1940–1946.

Lumsden, J.M., McCarty, T., Petiniot, L.K., Shen, R., Barlow, C., Wynn, T.A., Morse, H.C., 3rd, Gearhart, P.J., Wynshaw-Boris, A., Max, E.E., and Hodes, R.J. (2004). Immunoglobulin class switch recombination is impaired in Atm-deficient mice. J. Exp. Med. *200*, 1111–1121.

Maia, S., Haining, W.N., Ansen, S., Xia, Z., Armstrong, S.A., Seth, N.P., Ghia, P., den Boer, M.L., Pieters, R., Sallan, S.E., et al. (2005). Gene expression profiling identifies BAX-delta as a novel tumor antigen in acute lymphoblastic leukemia. Cancer Res. *65*, 10050–10058.

Mallette, F.A., Gaumont-Leclerc, M.F., and Ferbeyre, G. (2007). The DNA damage signaling pathway is a critical mediator of oncogene-induced senescence. Genes Dev. *21*, 43–48.

Matei, I.R., Gladdy, R.A., Nutter, L.M., Canty, A., Guidos, C.J., and Danska, J.S. (2007). ATM deficiency disrupts Tcra locus integrity and the maturation of CD4+CD8+ thymocytes. Blood *109*, 1887–1896.

McKinnon, P.J. (2004). ATM and ataxia telangiectasia. EMBO Rep. *5*, 772–776.

McNees, C.J., Conlan, L.A., Tenis, N., and Heierhorst, J. (2005). ASCIZ regulates lesion-specific Rad51 focus formation and apoptosis after methylating DNA damage. EMBO J. *24*, 2447–2457.

Muramatsu, M., Kinoshita, K., Fagarasan, S., Yamada, S., Shinkai, Y., and Honjo, T. (2000). Class switch recombination and hypermutation require activation-induced cytidine deaminase (AID), a potential RNA editing enzyme. Cell *102*, 553–563.

Neuberger, M.S., Harris, R.S., Di Noia, J., and Petersen-Mahrt, S.K. (2003). Immunity through DNA deamination. Trends Biochem. Sci. *28*, 305–312.

Nussenzweig, A., and Nussenzweig, M.C. (2010). Origin of chromosomal translocations in lymphoid cancer. Cell *141*, 27–38.

Oka, H., Sakai, W., Sonoda, E., Nakamura, J., Asagoshi, K., Wilson, S.H., Kobayashi, M., Yamamoto, K., Heierhorst, J., Takeda, S., and Taniguchi, Y.

(2008). DNA damage response protein ASCIZ links base excision repair with immunoglobulin gene conversion. Biochem. Biophys. Res. Commun. *371*, 225–229.

Petersen-Mahrt, S.K., Harris, R.S., and Neuberger, M.S. (2002). AID mutates *E. coli* suggesting a DNA deamination mechanism for antibody diversification. Nature *418*, 99–103.

Reina-San-Martin, B., Chen, H.T., Nussenzweig, A., and Nussenzweig, M.C. (2004). ATM is required for efficient recombination between immunoglobulin switch regions. J. Exp. Med. *200*, 1103–1110.

Reina-San-Martin, B., Nussenzweig, M.C., Nussenzweig, A., and Difilippantonio, S. (2005). Genomic instability, endoreduplication, and diminished Ig class-switch recombination in B cells lacking Nbs1. Proc. Natl. Acad. Sci. USA *102*, 1590–1595.

Revy, P., Muto, T., Levy, Y., Geissmann, F., Plebani, A., Sanal, O., Catalan, N., Forveille, M., Dufourcq-Labelouse, R., Gennery, A., et al. (2000). Activation-induced cytidine deaminase (AID) deficiency causes the autosomal recessive form of the Hyper-IgM syndrome (HIGM2). Cell *102*, 565–575.

Robbiani, D.F., Bunting, S., Feldhahn, N., Bothmer, A., Camps, J., Deroubaix, S., McBride, K.M., Klein, I.A., Stone, G., Eisenreich, T.R., et al. (2009). AID produces DNA double-strand breaks in non-Ig genes and mature B cell lymphomas with reciprocal chromosome translocations. Mol. Cell *36*, 631–641.

Saidi, A., Li, T., Weih, F., Concannon, P., and Wang, Z.Q. (2010). Dual functions of Nbs1 in the repair of DNA breaks and proliferation ensure proper V(D)J recombination and T-cell development. Mol. Cell. Biol. *30*, 5572–5581.

Savitsky, K., Bar-Shira, A., Gilad, S., Rotman, G., Ziv, Y., Vanagaite, L., Tagle, D.A., Smith, S., Uziel, T., Sfez, S., et al. (1995). A single ataxia telangiectasia gene with a product similar to PI-3 kinase. Science *268*, 1749–1753.

Schaffner, C., Stilgenbauer, S., Rappold, G.A., Dohner, H., and Lichter, P. (1999). Somatic ATM mutations indicate a pathogenic role of ATM in B-cell chronic lymphocytic leukemia. Blood *94*, 748–753.

Schaffner, C., Idler, I., Stilgenbauer, S., Dohner, H., and Lichter, P. (2000). Mantle cell lymphoma is characterized by inactivation of the ATM gene. Proc. Natl. Acad. Sci. USA *97*, 2773–2778.

Spring, K., Cross, S., Li, C., Watters, D., Ben-Senior, L., Waring, P., Ahangari, F., Lu, S.L., Chen, P., Misko, I., et al. (2001). Atm knock-in mice harboring an in-frame deletion corresponding to the human ATM 7636del9 common mutation exhibit a variant phenotype. Cancer Res. *61*, 4561–4568.

Spring, K., Ahangari, F., Scott, S.P., Waring, P., Purdie, D.M., Chen, P.C., Hourigan, K., Ramsay, J., McKinnon, P.J., Swift, M., and Lavin, M.F. (2002). Mice heterozygous for mutation in Atm, the gene involved in ataxia-telangiectasia, have heightened susceptibility to cancer. Nat. Genet. *32*, 185–190.

Stankovic, T., Stewart, G.S., Fegan, C., Biggs, P., Last, J., Byrd, P.J., Keenan, R.D., Moss, P.A., and Taylor, A.M. (2002). Ataxia telangiectasia mutated-deficient B-cell chronic lymphocytic leukemia occurs in pregerminal center cells and results in defective damage response and unrepaired chromosome damage. Blood *99*, 300–309.

Stilgenbauer, S., Winkler, D., Ott, G., Schaffner, C., Leupolt, E., Bentz, M., Moller, P., Muller-Hermelink, H.K., James, M.R., Lichter, P., and Dohner, H. (1999). Molecular characterization of 11q deletions points to a pathogenic role of the ATM gene in mantle cell lymphoma. Blood *94*, 3262–3264.

Stracker, T.H., Theunissen, J.W., Morales, M., and Petrini, J.H. (2004). The Mre11 complex and the metabolism of chromosome breaks: the importance of communicating and holding things together. DNA Repair (Amst.) *3*, 845–854.

Uziel, T., Lerenthal, Y., Moyal, L., Andegeko, Y., Mittelman, L., and Shiloh, Y. (2003). Requirement of the MRN complex for ATM activation by DNA damage. EMBO J. *22*, 5612–5621.

Wang, J.H., Gostissa, M., Yan, C.T., Goff, P., Hickernell, T., Hansen, E., Difilippantonio, S., Wesemann, D.R., Zarrin, A.A., Rajewsky, K., et al. (2009). Mechanisms promoting translocations in editing and switching peripheral B cells. Nature *460*, 231–236.

Xu, Y., and Baltimore, D. (1996). Dual roles of ATM in the cellular response to radiation and in cell growth control. Genes Dev. *10*, 2401–2410.

Xu, Y., Ashley, T., Brainerd, E.E., Bronson, R.T., Meyn, M.S., and Baltimore, D. (1996). Targeted disruption of ATM leads to growth retardation, chromosomal fragmentation during meiosis, immune defects, and thymic lymphoma. Genes Dev. *10*, 2411–2422.